

## RESEARCH ARTICLE SUMMARY

## NEUROSCIENCE

## A neural basis for prosocial behavior toward unresponsive individuals

Fangmiao Sun, Ye Emily Wu\*, Weizhe Hong\*

**INTRODUCTION:** The partial or complete loss of responsiveness, such as transient unconsciousness, presents a substantial risk to animals, increasing their vulnerability to predators or hazardous environments. The actions of bystanders toward unresponsive individuals can be critical for enhancing survival and well-being. Humans, for instance, can readily recognize and assist unconscious individuals. Similarly, anecdotal reports suggest that some animal species, including nonhuman primates, marine mammals (e.g., whales and dolphins), and elephants, exhibit behavioral reactions to collapsed or unresponsive conspecifics in the wild. However, it is unclear whether such behaviors occur in species beyond those few that have been documented. Additionally, the nature, characteristics, and consequences of these behaviors have not been systematically examined in a controlled experimental setting. Moreover, the neural mechanisms underlying the per-

ception of others' unresponsive states and the ensuing behaviors remain elusive.

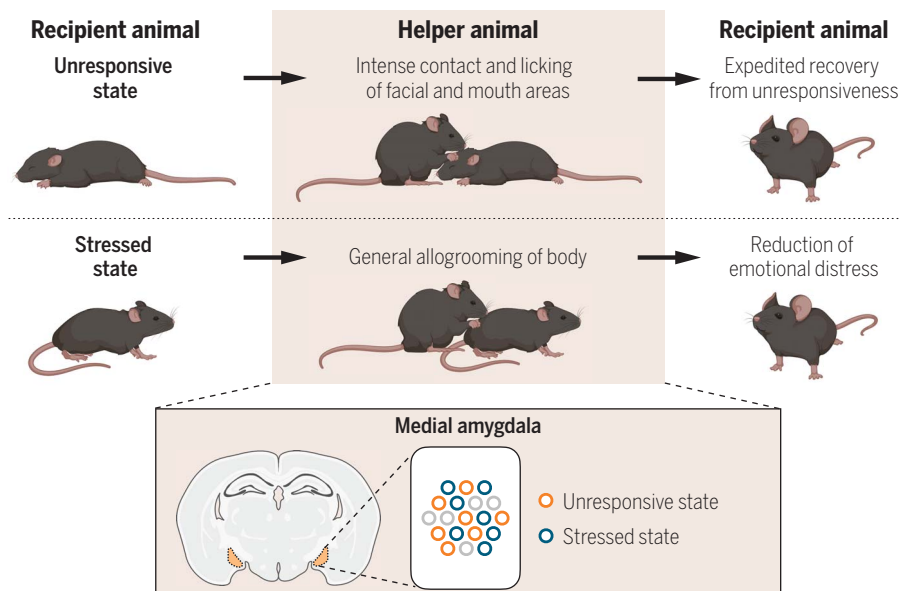
**RATIONALE:** Previous studies have demonstrated that rodents, including mice, can perceive and behaviorally respond to others' negative or needy states. For example, they can display comforting social touch through allogrooming, broadly targeted at various body parts of distressed conspecifics. In addition, they can respond to others' local pain and injury with allolicking behavior focused on the wound site. However, it is unclear how mice react to other animals in an unresponsive state. In this study, we examined the behaviors that mice display toward unresponsive conspecifics, their effects on the recipients, and the neural representation and regulation of these behaviors.

**RESULTS:** We discovered that mice preferentially approach unresponsive conspecifics over

awake ones and engage in distinctive behaviors toward unresponsive conspecifics under deep sedation, characterized by intense contact and grooming directed at the sedated individuals' head region, particularly the facial and mouth areas. These behaviors are observed in both male and female animals and are correlated with the extent of reduction in the responsiveness of the recipients. Physical contact and grooming directed at the head region are more likely to elicit motor responses in the recipients compared with other social behaviors and can expedite the animals' recovery from the unresponsive state.

Moreover, we uncovered an essential role of the medial amygdala (MeA) in regulating this response. MeA neural activity differentiates between awake and sedated conspecifics at both single-cell and population levels, and the neural response to sedated animals does not simply reflect a response to novelty. Optogenetic silencing of MeA  $\gamma$ -aminobutyric acid-producing (GABAergic) neurons suppresses head grooming behavior, whereas their activation promotes this behavior. Although mice respond to sedated, unresponsive conspecifics primarily with head-directed allogrooming and physical contact, their allogrooming response to awake conspecifics experiencing a general state of stress mainly targets other body regions. These two different adverse states and the corresponding behavioral responses (head grooming versus body grooming) are distinguishable by neural activities in the MeA, suggesting that the MeA may be part of the neural circuitry mediating the differentiation between these states.

**CONCLUSION:** Our findings reveal that mice exhibit rescue-like behaviors toward unresponsive conspecifics, characterized by intense physical contact directed at the recipient's head region. This response accelerates recovery from unresponsiveness, potentially reducing risks to unresponsive individuals and enhancing their survival. We have also uncovered that the MeA encodes the unresponsive state of others and drives head-directed grooming toward them. Notably, the behavioral response toward unresponsive conspecifics differs from that toward awake, stressed individuals, and these responses are differentially represented in the MeA. These findings shed light on the neural mechanisms underlying prosocial responses toward unresponsive individuals, broadening our understanding of animals' ability to detect and behaviorally react to different adverse conditions of others. ■



**Prosocial behavior toward unresponsive conspecifics.** Mice can detect the unresponsive state of other individuals and exhibit rescue-like behavior characterized by intense physical contact directed at the recipient's head region, which facilitates recovery from unresponsiveness. Neural activity in the medial amygdala (MeA) encodes the unresponsive state of others and regulates the ensuing prosocial actions. The behavior exhibited toward unresponsive conspecifics differs from that directed toward stressed individuals, and these interactions are differentially represented in the MeA. [Figure created with BioRender.com]

The list of author affiliations is available in the full article online.

\*Corresponding author. Email: whong@ucla.edu (W.H.); ye.wu@ucla.edu (Y.E.W.)

Cite this article as F. Sun, et al., *Science* 387, eadq2679 (2025). DOI: 10.1126/science.adq2679

**READ THE FULL ARTICLE AT**  
<https://doi.org/10.1126/science.adq2679>

## RESEARCH ARTICLE

## NEUROSCIENCE

## A neural basis for prosocial behavior toward unresponsive individuals

Fangmiao Sun<sup>1,2</sup>, Ye Emily Wu<sup>1,2\*</sup>, Weizhe Hong<sup>1,2,3\*</sup>

Humans often take actions to assist others experiencing unresponsiveness, such as transient loss of consciousness. How other animals react to unresponsive conspecifics—and the neural mechanisms driving such behaviors—remain largely unexplored. In this study, we demonstrated that mice exhibit rescue-like social behaviors toward unresponsive conspecifics, characterized by intense physical contact and grooming directed at the recipient's facial and mouth areas, which expedite their recovery from unresponsiveness. We identified the medial amygdala (MeA) as a key region that encodes the unresponsive state of others and drives this head-directed physical contact. Notably, the behavioral responses toward unresponsive conspecifics differed from those directed at awake, stressed individuals, and these responses were differentially represented in the MeA. These findings shed light on the neural mechanisms underlying prosocial responses toward unresponsive individuals.

Experiencing a partial or complete loss of responsiveness, such as a transient loss of consciousness, poses a danger to animals because it may lead to increased exposure to predators or harmful environments. The ability of bystanders to attend to partially or completely unresponsive individuals can thus play a vital role in promoting animal survival and well-being. Humans can readily recognize other individuals' unconscious states and provide aid (1). In addition, there have been sporadic, anecdotal observations of behavioral reactions toward collapsed or unresponsive conspecifics in the wild in other animal species, such as nonhuman primates, marine mammals (whales and dolphins), and elephants (2–6). These prosocial behaviors, which may include staying in proximity, sniffing, licking, grooming, carrying, and dragging, could reflect attentive and affiliative responses to the collapsed individuals under some circumstances. However, it remains unclear whether such phenomena exist in species beyond those few that have been documented. Furthermore, the nature, characteristics, and consequences of actions toward unresponsive conspecifics have not been systematically examined in a controlled experimental setting, and the underlying neural mechanisms remain elusive. Previous studies have demonstrated that rodents, including mice, can perceive and behaviorally respond to others' negative or needy states (7–13). In particular, they can display comforting behavior through

allogrooming, a form of affiliative social touch, broadly targeted at various body parts of distressed conspecifics (7). In addition, they can respond to others' local pain and injury with allolicking behavior focused on the wound site (8). However, it is unclear how mice respond to other animals in an unresponsive state.

In this study, we show that mice exhibit a distinctive set of behaviors toward unresponsive conspecifics, characterized by intense physical contact, including grooming and licking behaviors, that is targeted at the facial and mouth areas of the recipient. These behaviors, which are induced by the unresponsive state in other animals, could expedite recovery from such a state, suggesting a potential rescue-like role of these behaviors in enhancing group survival. Lastly, we show that the medial amygdala (MeA) encodes the unresponsive state of others and is required for behavioral responses to this state.

### Results

#### Prosocial behavioral responses toward unresponsive social partners

To explore how mice respond to unresponsive conspecifics, we induced a deep-sedation state (14) in mice through injection of a sedative, dexmedetomidine. The concept of sedation encompasses a continuum of responsiveness levels, ranging from minimal sedation equivalent to anxiolysis, to light and moderate sedation in which individuals display reduced responsiveness, to deep sedation in which individuals cannot be easily aroused but may respond to intense stimuli, and to the deepest sedation equivalent to general anesthesia (14). Under the deep-sedation condition in our experiments, mice exhibited minimal responsiveness, remaining mostly immobile and displaying only subtle movements in response to strong external stimuli (hereafter referred to as an

“unresponsive” state). We then examined direct interactions between naïve animals (helpers) and their cohoused partners (recipients) that were either awake or unresponsive (Fig. 1A). We observed that helper animals exhibited a significantly higher amount of time spent in grooming and intense physical contact (collectively referred to as allogrooming) toward unresponsive partners compared with awake partners (Fig. 1B). This increase in allogrooming was observed in both male (Fig. 1, B to P, and fig. S1) and female helper animals (Fig. 1Q and fig. S2), with comparable amounts in both groups (Fig. 1, R to T). By contrast, the total duration of social investigation toward awake and unresponsive partners was comparable (Fig. 1G and fig. S2B). We performed further analysis to identify the body parts of the recipient that were most frequently groomed by the helpers and found that the trunk (particularly dorsal flank and neck) and head regions were the main target areas (Fig. 1, F, and I to M). Compared with other body parts, the head regions, particularly the facial and mouth areas of the recipients, received the majority of allogrooming (Fig. 1, F, and M to P; and figs. S1, S2A, and S2H to S2K). By contrast, self-directed grooming in helper animals did not increase during the same period (Fig. 1H, and figs. S1F and S2C), arguing against a nonspecific increase in generic grooming behavior. To examine whether the sex of the partners could influence the behavior of the helpers, we performed experiments using male helpers paired with female recipients and female helpers paired with male recipients. We found that the amount of head grooming behavior toward male and female recipients did not significantly differ in either male or female helpers (fig. S3).

We further examined how individual behaviors emerge as the partners transition from an awake to an unresponsive state. We found that helper mice initially displayed a substantial amount of investigation behavior before the onset of the sedated state (Fig. 2, A, B, and E). Investigation behavior was subsequently reduced after the partners' transition to the sedated state (Fig. 2, A, B, and E), and this was accompanied by an increased time spent in head grooming (Fig. 2, A, C, D, F, and G). We further examined how allogrooming behavior targeted at different body parts of the recipients correlates with the depths of sedation in recipient mice (Fig. 2H). We found that a deeper sedated state in recipient mice elicited a greater amount of head grooming (in particular mouth contact) compared with mice in a lighter sedated state (Fig. 2, H, and I to N), whereas the amount of time spent in social investigation, self-grooming, or body grooming was not different (Fig. 2, I to K). Together, our findings suggest that head grooming is a prominent behavior response induced by others' loss of responsiveness in mice.

<sup>1</sup>Department of Neurobiology, David Geffen School of Medicine, University of California, Los Angeles, Los Angeles, CA, USA. <sup>2</sup>Department of Biological Chemistry, David Geffen School of Medicine, University of California, Los Angeles, Los Angeles, CA, USA. <sup>3</sup>Department of Bioengineering, Samueli School of Engineering, University of California, Los Angeles, Los Angeles, CA, USA.

\*Corresponding author. Email: whong@ucla.edu (W.H.); ye.wu@ucla.edu (Y.E.W.)

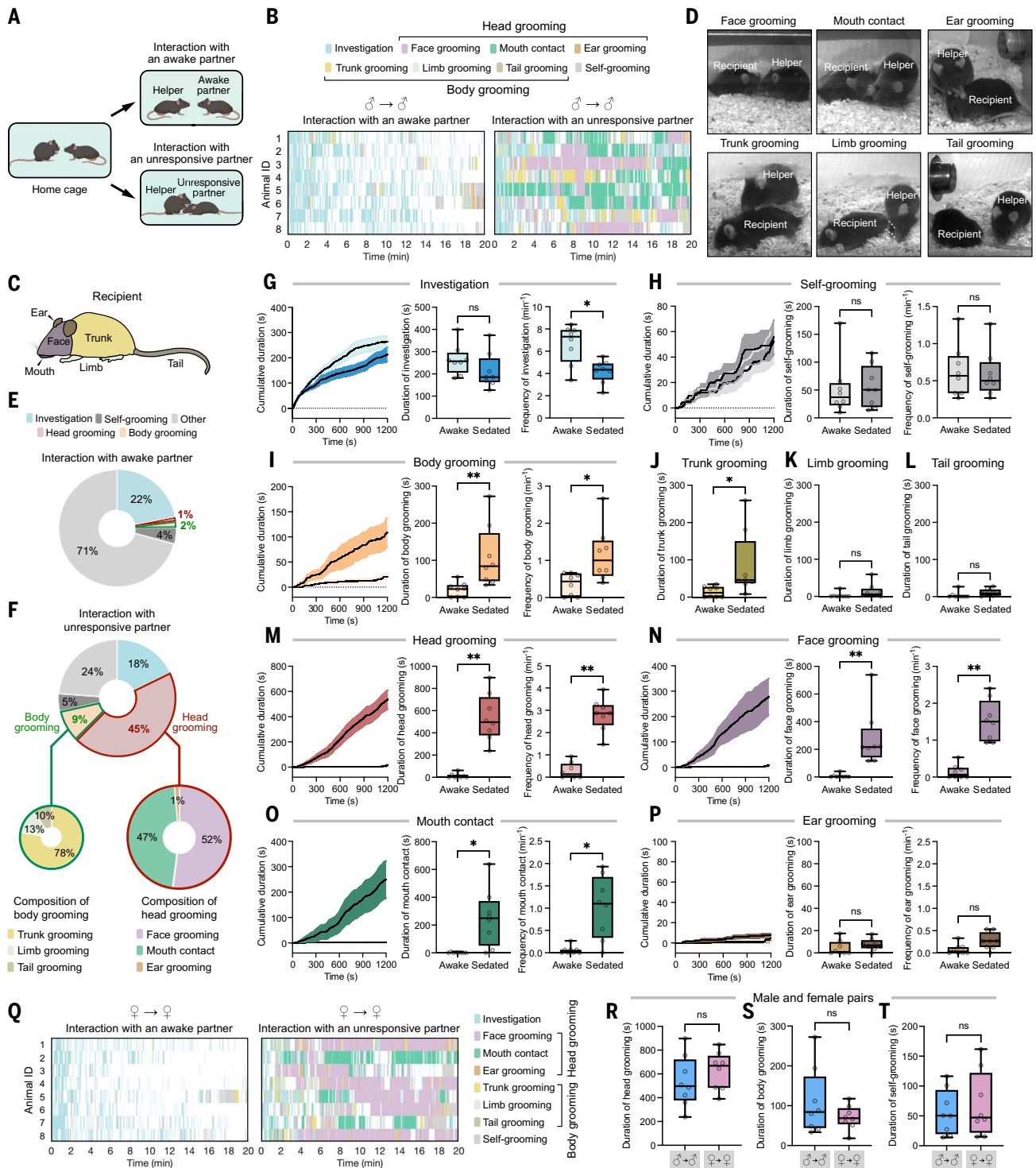


**Fig. 1. Behavioral responses toward unresponsive conspecifics in mice.**

(A) Schematic of the experimental paradigm. Naive helpers interacted with either awake partners or unresponsive (sedated) partners. (B) Example raster plots showing social investigation, head grooming, body grooming, and self-grooming behaviors exhibited by male helper animals during interaction with awake or sedated male partners. Each numbered row represents an individual animal. (C) Schematic of different body parts of the partner that received allogrooming by the helper. (D) Example video frames showing allogrooming directed at the facial, mouth, and other body areas of sedated partners (recipients). Dashed lines in limb grooming indicate the limb

position. (E and F) The percentage of time that male helper animals spent in different behaviors during interactions with awake or sedated male partners or during grooming behaviors directed at various head or body areas of male sedated partners. (G to I) and (M to P) The time courses of cumulative duration (mean ± SEM; left), total duration (middle), and frequency (right) of social investigation, self-grooming, body grooming, head grooming, face grooming, mouth contact, and ear grooming behaviors displayed by male helper animals during interactions with awake or sedated male partners. (J to L) Duration of grooming behavior directed at the trunk, limbs, and tail of the partners. (Q) Example raster plots showing social investigation, head

grooming, body grooming, and self-grooming behaviors exhibited by female helper animals during interaction with awake or sedated female partners. Each numbered row represents an individual animal. **(R to T)** Comparison of the total durations of head grooming, body grooming, and self-grooming displayed by male

versus female helpers during interactions with same-sex sedated partners.  $n = 8$  male mice in (G) to (P);  $n = 8$  male mice and 8 female mice in (R) to (T). For (G) to (P), two-sided Wilcoxon signed-rank test; for (R) to (T), two-sided Wilcoxon rank-sum test.  $***P < 0.01$ ,  $**P < 0.05$ ; ns, not significant.

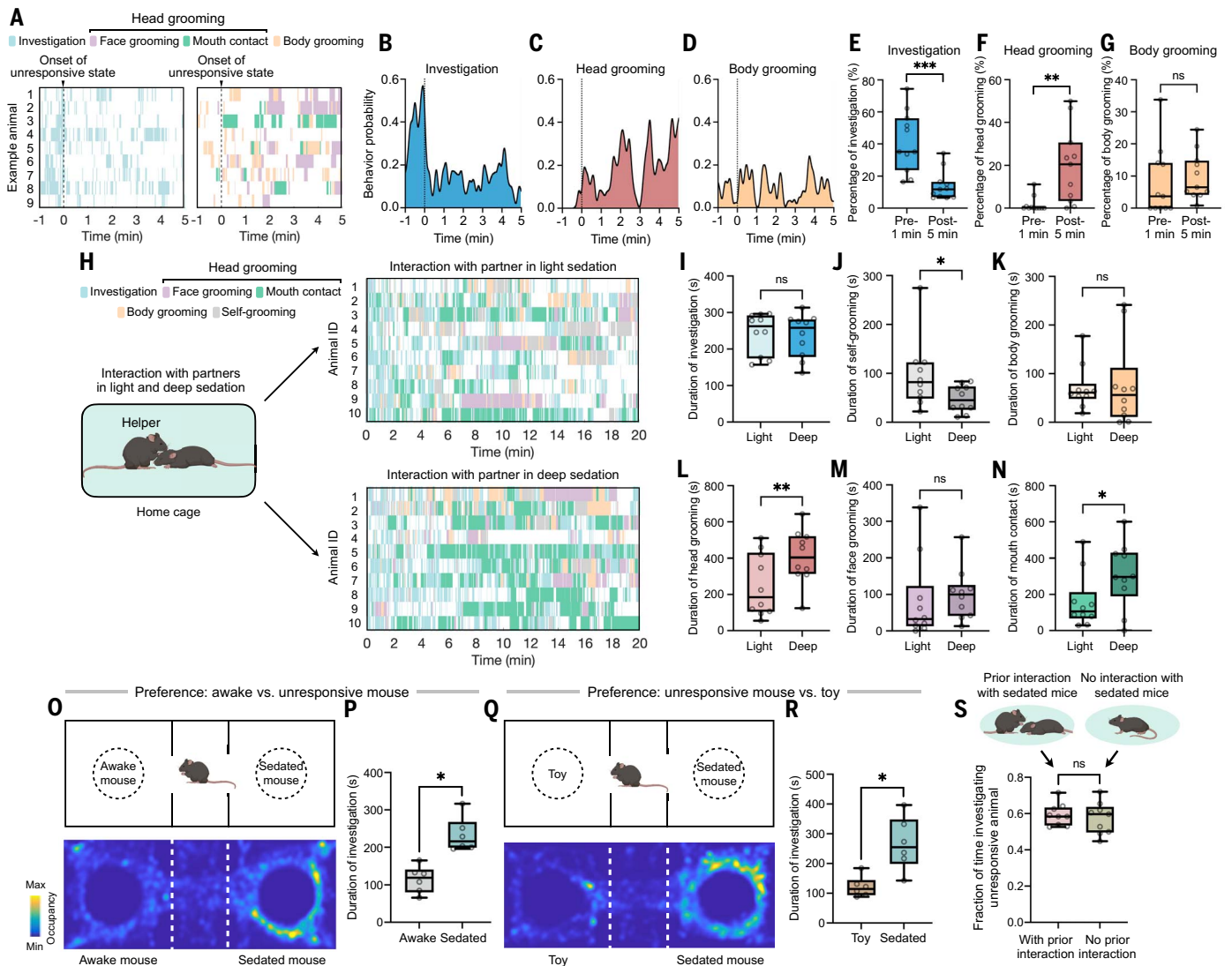


**Fig. 2. Head grooming toward partners correlates with reduction in their responsiveness.** **(A)** Example raster plots showing social investigation, head grooming, and body grooming behaviors displayed by helper animals as partners transitioned from the awake state to the sedated state. **(B to D)** The probability of helper animals displaying social investigation (B), head grooming (C), or body grooming (D) toward partners at different time points during the 1 min before or 5 min after the onset of the sedated state in the partners (time 0). **(E to G)** Percentage of time that helper animals displayed social investigation (E), head grooming (F), or body grooming (G) toward partners during the 1 min before or 5 min after the onset of the sedated state in the partners. **(H)** Schematic and example raster plots showing various types of behaviors displayed by helper animals during interactions with partners in light or deep sedation. **(I to N)** Duration of

various behaviors exhibited by helper animals during interactions with partners in light versus deep sedation. **(O and Q)** (Top) Schematic of the three-chamber tests for assessing the helper animals' preference for an awake versus sedated partner (O) or a sedated partner versus a toy mouse (Q). (Bottom) Example heatmaps showing the animals' occupancy at different locations in the chambers. **(P and R)** The total duration of investigation toward an awake versus sedated partner (P) or a sedated partner versus a toy mouse (R). **(S)** The fraction of time that helper animals spent investigating awake or sedated partners after prior interaction with the sedated partners.  $n = 11$  mice in (E) to (G);  $n = 10$  mice in (I) to (N);  $n = 6$  mice in (P) to (R);  $n = 9$  mice in each group in (S). For (E) to (G); (I) to (N); and (P), (R), and (S), two-sided Wilcoxon signed-rank test was performed.  $***P < 0.001$ ,  $**P < 0.01$ ,  $*P < 0.05$ ; ns, not significant.

### Mice show a positive preference toward unresponsive partners

Although we found that mice displayed allogrooming behavior toward an unresponsive

partner, it is possible that helper mice may not voluntarily choose to attend to an unresponsive animal if they have a choice of interacting with an awake animal. We therefore examined

whether animals display a positive preference for a sedated partner over an awake partner when both are present. To this end, we performed a three-chamber preference test, in

which a mouse chose to interact with a target mouse that was either sedated or awake (Fig. 2O). Mice spent more time approaching a sedated mouse compared with an awake mouse (Fig. 2P), suggesting that interactions with sedated animals were not due to the absence of awake animals to interact with but instead reflected a genuine positive preference to attend to sedated individuals. We found that the animals showed a similar positive preference for familiar and novel sedated animals over awake mice (fig. S4, A and B), suggesting that the novelty of the individuals did not significantly affect the preference for sedated animals.

One potential explanation for this preference is that the sedated state may simply be perceived as a novel signal. To assess whether this preference was merely driven by the novelty of the sedated state, we performed another set of experiments in which the helper animal was first allowed to freely interact with a sedated animal before undergoing the three-chamber test with the same sedated animal (fig. S4C). We found that prior interaction with the sedated animal did not reduce the helper animal's preference for the same sedated mouse (Fig. 2S and fig. S4D), suggesting that this preference is unlikely driven by the novelty of the sedated state.

We further investigated how familiarity affects behaviors during free interactions with sedated animals. We found that the amount of time spent in head grooming and body grooming behaviors toward sedated animals was not significantly different between familiar pairs and unfamiliar pairs (fig. S4, E to I), suggesting that these behaviors are not critically dependent on the familiarity between the interacting mice in this context.

Moreover, a major distinction between sedated and awake mice was that sedated mice were stationary. To rule out the possibility that animals simply prefer to interact with inanimate objects, we tested animals in a three-chamber with the choices of a sedated mouse and a stationary toy mouse (Fig. 2Q). We found that mice spent more time investigating a sedated mouse compared with the toy mouse (Fig. 2R), suggesting that the preference was not for a stationary object but rather for a sedated conspecific.

#### **Head-directed allogrooming facilitates recipients' recovery from an unresponsive state**

When animals were under sedation, they occasionally displayed tail twitching (Fig. 3A), which may reflect a response to external stimuli when sensory inputs are strong. We found that when sedated animals were placed with helper mice, they displayed an increased amount of tail-twitching bouts (Fig. 3, B and C). In particular, a majority of tail-twitching behavior occurred when the helper mice engaged in head grooming toward the recipients (Fig. 3D), and there was a positive correlation between the number of tail-twitching bouts and the dura-

tion of mouth contact (Fig. 3E); no correlation was found with time spent in investigation (Fig. 3F). This suggests that head grooming may provide strong sensory inputs to the sedated mice, leading to an increased motor response.

On the basis of these observations, we hypothesized that head grooming may facilitate the recovery from the sedated state. We therefore examined the amount of time that sedated animals took to recover from an unresponsive state in the presence or absence of a cage mate (Fig. 3G). During deep sedation, the animals remained largely immobile, staying in one location in either a lying or crouching posture. As they gradually transitioned to wakefulness, they began to return to a standing position, displayed minor movements, and eventually resumed continuous activity. We found that sedated animals accompanied by a cage mate recovered faster from the unresponsive state (materials and methods) compared with those that were alone (Fig. 3H), indicating that the presence of the cage mates accelerated the recovery of sedated animals from the unresponsive state. Around the time that partners transitioned to wakefulness, we found that the helper animals reduced the time spent in head grooming toward their partners compared with the earlier phase of their interactions (when the partner was sedated; fig. S5A). This is likely because partner animals were in a light sedation state as they were resuming wakefulness and is consistent with our observation that animals exhibited less head grooming toward lightly sedated animals compared with those under deep sedation (Fig. 2, H to N).

Lastly, we examined how helper animals may detect the unresponsive state of the sedated animals. To test whether visual cues are required, we performed an experiment under complete darkness and compared it with those performed under white-light illumination. We found that helper animals showed comparable time spent in investigation and head grooming behaviors toward unresponsive mice under white-light illumination and in complete darkness (fig. S5, B to F). This suggests that visual inputs are not indispensable for detecting the unresponsive state of the sedated animals and that other sensory modalities, such as olfactory or somatosensory cues, are likely involved. To rule out the possibility that head grooming behavior may be simply induced by the odor from the sedative itself or the experimenter, we applied the sedative over the partners' bodies instead of injecting it. We found that this led to minimal head grooming behavior by the helper mice (total duration:  $2.8 \pm 1.4$  s, mean  $\pm$  SEM). Additionally, partners injected with saline elicited little head grooming from the helpers (Fig. 1, M to P). These results suggest that head grooming behavior toward sedated animals was unlikely to be induced by the odor of the sedative itself or the exper-

imenter but may instead have involved other signals from the sedated animals.

#### **Neural representations of unresponsive partners and behavioral responses toward them in the MeA**

In mice, olfactory and pheromonal cues are the primary sensory cues for the detection of the social environment (15). The MeA is a hub brain region in processing and integrating social inputs from the olfactory and pheromonal systems and is involved in regulating various social behavioral outputs (16–21). To investigate whether and how MeA neurons may encode the unresponsive state of other individuals, we used in vivo microendoscopic calcium imaging during free interaction with sedated conspecifics (Fig. 4A). We expressed the fluorescence calcium indicator jRCaMP7f (22) in MeA neurons and implanted a gradient refractive index (GRIN) lens above the MeA (Fig. 4, B and C). During imaging sessions, we sequentially presented each helper animal with awake and sedated conspecifics, and the animals were allowed to freely interact. Calcium fluorescence videos were processed by using a constrained nonnegative matrix factorization algorithm (CNMF-E) (23) to identify single cells and extract their calcium signals (Fig. 4C and movie S1).

Using a receiver-operating characteristic (ROC) analysis (7, 24), we first identified neurons that were significantly active during social investigation toward awake or sedated conspecifics. We found that 28.5% of MeA neurons exhibited significant activation in response to sedated individuals (Fig. 4D). These neurons partially overlapped with neurons activated by awake animals (Fig. 4, D and E), possibly reflecting common sensory cues shared by both types of social targets. However, a subset of these neurons was activated selectively by sedated animals but not awake ones (Fig. 4, D to H, and fig. S6A). Similarly, we identified another subpopulation of neurons that exhibited increased activity in response to awake animals but not sedated ones (Fig. 4, D to H, and fig. S6A). Furthermore, linear classifiers constructed by using population activity could decode awake versus sedated conspecifics with high performance (Fig. 4I), indicating that these two types of social targets are reliably discernible within high-dimensional activity spaces. These results suggest that MeA neural activity can distinguish between the awake and unresponsive states of others at both single-cell and ensemble levels.

We further examined MeA neuronal responses during head grooming behavior toward sedated conspecifics and found that 24.7% of MeA neurons were significantly activated during this behavior (Fig. 4, J and K). We next asked whether head grooming and body grooming are associated with similar or different neural representations in the MeA. We found

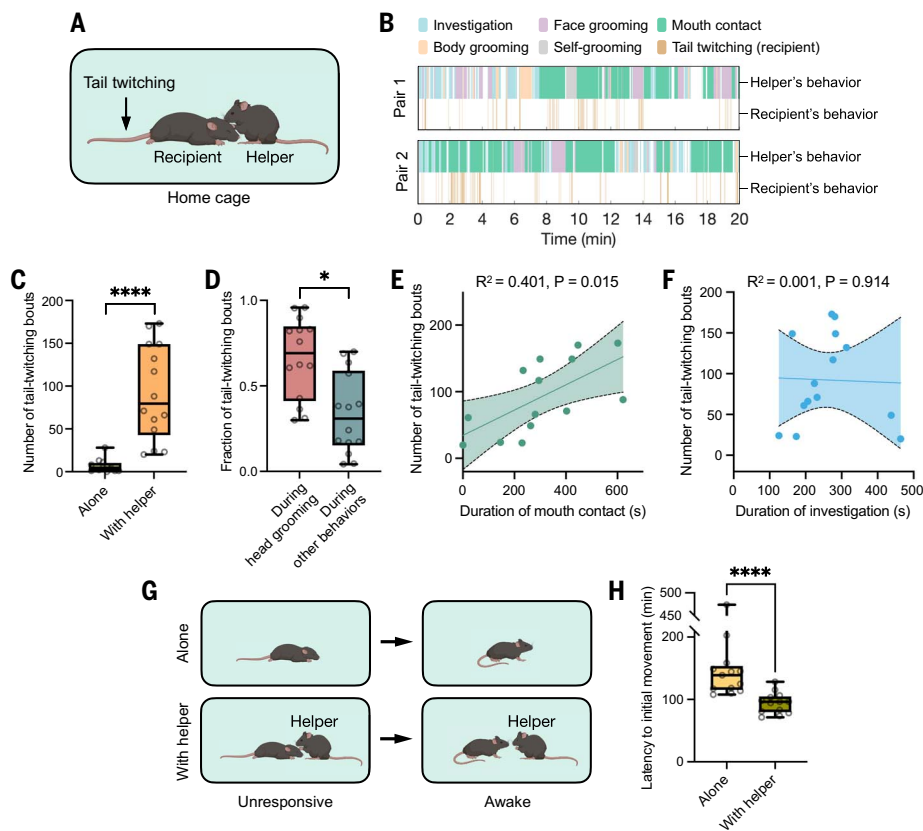


**Fig. 3. Head grooming toward partners accelerates recovery from a sedated state. (A and B)**

Schematic (A) and example raster plots (B) showing tail movements of sedated animals during various behaviors of helper animals. (C) The number of tail-twitching bouts of sedated animals when they were alone or placed with helper animals. (D) The fraction of tail-twitching bouts of sedated animals that occurred during head grooming versus other types of behaviors of the helper animals. (E and F) The correlation between the duration of mouth contact (E) or social investigation (F) of helper animals and the number of tail movement bouts of sedated animals.  $R^2$ , coefficient of determination. (G and H) Schematic and quantification of the amount of time that it took for partner animals to recover from the sedated state when they were alone or placed with helpers.  $n = 12$  mice in the “alone” group and 14 mice in the “with helper” group in (C);  $n = 14$  mice in (D) to (F);  $n = 13$  mice in each group in (H). For (C) and (H), two-sided Wilcoxon rank-sum test; for (D), two-sided Wilcoxon signed-rank test; for (E) and (F), linear regression. \*\*\*\* $P < 0.0001$ , \* $P < 0.05$ .

that neurons activated during these two behaviors showed partial overlap (Fig. 4, J and K). However, a sizable fraction of head grooming-activated neurons did not respond during body grooming, and vice versa (Fig. 4, J to N, and fig. S6B). Moreover, these two behaviors could be decoded using population activity with accuracy exceeding chance levels (Fig. 4O). Decoding analysis using neural activity at different time points relative to behavior onset showed that the decodability between these two behaviors rose above chance and peaked shortly after behavior onset (Fig. 4P). These results suggest that head grooming and body grooming are associated with different neural representations in the MeA.

We further investigated the relationship between cells activated during head grooming and those activated during investigation toward sedated or awake conspecifics. We found that

a subset of neurons responded during all three types of events (Fig. 4Q), possibly reflecting general social cues common to these events. However, we also identified cells that responded during head grooming and sedated animal investigation but not during awake animal investigation (Fig. 4, Q and S). The overlap between head grooming cells and those responsive during sedated animal investigation was significantly above the chance level (Fisher’s exact test, odds ratio = 4.4,  $P < 0.0001$ ) and markedly higher than the overlap between head grooming cells and awake animal investigation cells (Fisher’s exact test, odds ratio = 3.3,  $P = 0.0016$ ), which was at chance level (Fisher’s exact test, odds ratio = 1.3,  $P = 0.48$ ) (Fig. 4R). This suggests that some cells responsive to sedated animals might be recruited to promote head grooming behavior. Additionally, we identified cells that were selectively activated during head

grooming but not during investigation toward either sedated or awake animals (Fig. 4, Q, T, and U, and fig. S6C), suggesting that MeA neural responses during head grooming do not merely reflect sensory sampling.

Our behavioral experiments indicate that prior interaction with the sedated animal did not reduce the helper animal’s preference to approach the same sedated animal. This suggests that this preference is not simply due to the novelty of the sedated state (Fig. 2S). To further examine whether MeA neural activity also encodes social novelty and whether the encoding of novel conspecifics differs from the encoding of sedated conspecifics, we performed microendoscopic imaging while helper mice interacted with awake or sedated conspecifics that were either familiar or novel (Fig. 4V). We found that familiar and novel awake animals activated partially distinct cell populations in the MeA and could be decoded using MeA population activity (fig. S6, D and E), suggesting that MeA neural responses differ between familiar and novel animals. We further compared cells activated by familiar sedated animals and those activated by novel awake animals. A substantial fraction of cells that responded to familiar sedated animals did not show increased activity in response to novel awake animals, and vice versa (Fig. 4, W to Y). This suggests that these two types of conspecifics (sedated versus novel) elicited partially distinct responses at the single-cell level. At the population level, we found that investigation events toward familiar sedated animals and novel awake animals could be reliably classified using ensemble neural activity (fig. S6F). These results suggest that sedated animals were not merely perceived as novel animals.

Lastly, we examined whether MeA neural activity in helper animals could encode the awake versus sedated state of novel (unfamiliar) partners. We found that a subset of cells activated by unfamiliar sedated animals were not activated by unfamiliar awake animals, and vice versa (fig. S6, G to I). Additionally, investigation events toward unfamiliar sedated animals versus unfamiliar awake animals could be distinguished by using population neural activity (fig. S6J). These results suggest that MeA neural activity can encode the awake versus sedated state in novel recipients, which is consistent with our observation that animals can differentiate between the sedated versus awake states in both familiar and novel conspecifics (fig. S4, A and B).

#### MeA GABAergic neurons control head grooming behavior toward unresponsive partners

We further examined whether the MeA plays a causal role in regulating allogrooming behavior toward unresponsive animals. As  $\gamma$ -aminobutyric acid-producing (GABAergic) (Vgat<sup>+</sup>) neurons

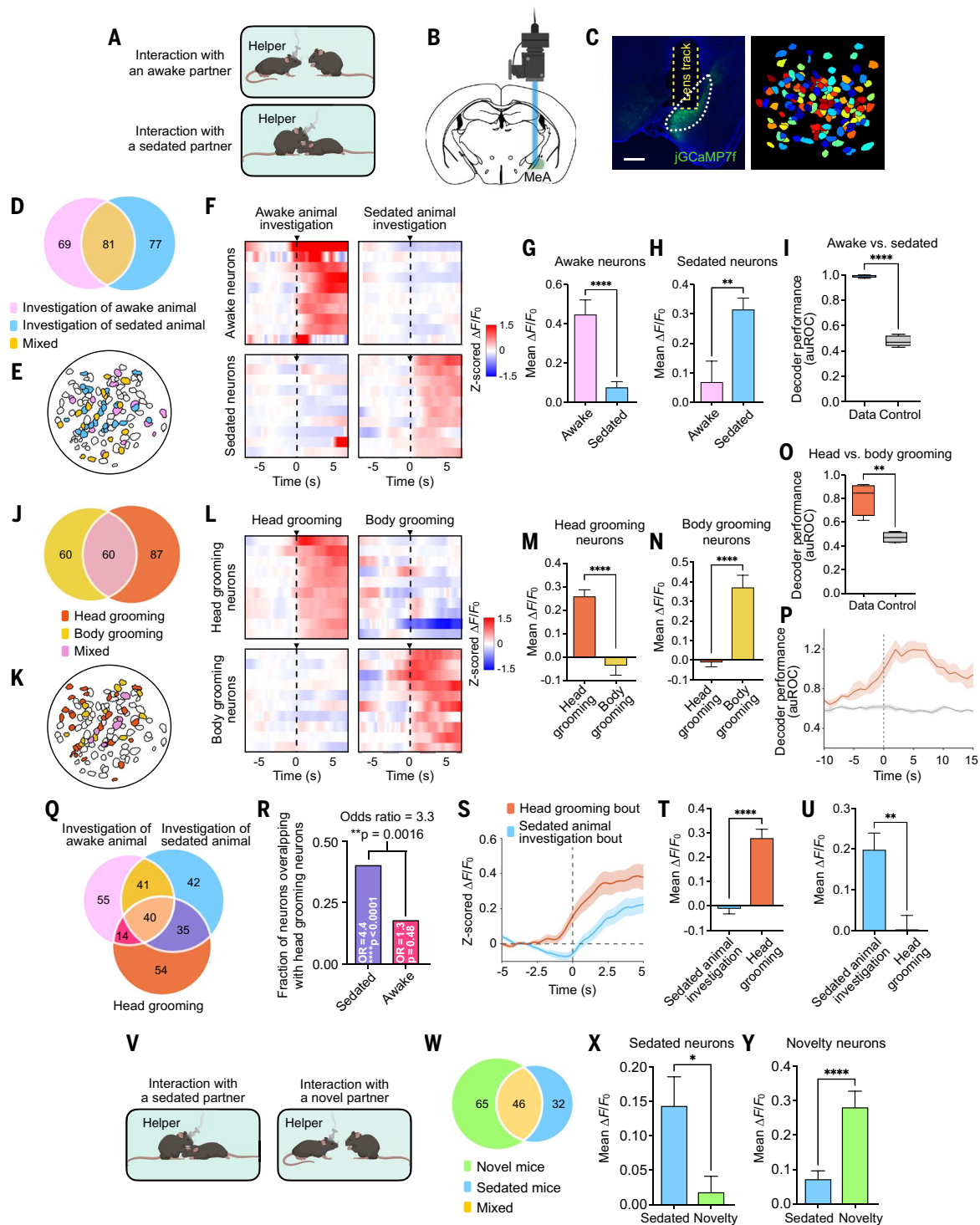


**Fig. 4. MeA neural activity encodes interactions with unresponsive conspecifics.** (A) Schematic of microendoscopic imaging during interactions with awake or sedated conspecifics. (B) Illustration of head-mounted microendoscope and GRIN lens implantation above the MeA. (C) (Left) Example image showing viral expression and GRIN lens implantation in the MeA. Scale bar, 500  $\mu\text{m}$ . (Right) ROIs (regions of interest) corresponding to single neurons extracted from an example field of view. (D, J, and Q) Venn diagrams showing the overlap and difference between neurons activated during social investigation toward either awake or sedated partners (D); between neurons activated during either head grooming or body grooming toward sedated partners (J); and between

neurons activated during either investigation toward awake partners, investigation toward sedated partners, or head grooming toward sedated partners (Q). (E and K) Example field of views illustrating the spatial distribution of cell types shown in (D) and (J), respectively. (F and L) Heatmaps showing average responses of example neurons activated selectively during investigation of either awake ("Awake neurons") or sedated ("Sedated neurons") partners but not both (F), and example cells activated selectively during either head grooming or body grooming toward sedated partners but not both (L). Activity data were aligned to the onset (time 0) of investigation (F) or allogrooming (L) behavior. (G and H) Average activity changes (mean  $\pm$  SEM) of cells selectively activated

by either awake (G) or sedated (H) partners during investigation toward each type of partner. **(I)** Performance of support vector machine (SVM) decoders in classifying investigation events toward awake versus sedated partners. **(M and N)** Average activity changes (mean  $\pm$  SEM) of cells selectively activated during either head grooming (M) or body grooming (N) toward sedated partners for each type of behavior. **(O)** Performance of SVM decoders in classifying head grooming versus body grooming toward sedated partners. **(P)** Time course (mean  $\pm$  SEM) of the performance of SVM decoders trained using population activities at different time points relative to behavior onset in classifying head grooming versus body grooming toward sedated partners. **(R)** Fractions of cells that overlap with head grooming cells among those selectively activated during either sedated animal investigation or awake animal investigation (but not both). The odds ratios (OR) and *P* values on each bar indicate the significance of the overlap between head grooming cells and cells activated during investigation toward sedated or awake animals. The OR and *P* value between the bars indicate the relative enrichment of head grooming cells among those activated during the investigation of sedated animals compared with those activated during the investigation of awake animals. **(S)** Average activity traces (mean  $\pm$  SEM) of cells activated during both head grooming and investigation toward sedated partners for each type of

behavior. Time 0 represents the onset of behavior events. **(T and U)** Average activity changes (mean  $\pm$  SEM) of cells selectively activated during either head grooming (T) or sedated animal investigation (U) for each type of behavior. **(V)** Schematic of microendoscopic imaging during interactions with familiar sedated or novel awake conspecifics. **(W)** Venn diagram showing the overlap and difference between neurons activated during social investigation toward either novel awake animals or familiar sedated animals. **(X and Y)** Average activity changes (mean  $\pm$  SEM) of cells selectively activated during social investigation toward either familiar sedated (X) or novel awake (Y) animals (but not both) for each type of behavior. Time 0 represents the onset of investigation events. *n* = 551 total neurons from 6 mice in (D) and 594 total neurons from six mice in (J); *n* = 69 awake partner-activated cells in (G) and 77 sedated partner-activated cells in (H); *n* = 5 mice in (I); *n* = 60 body grooming-activated cells in (M) and 87 head grooming-activated cells in (N); *n* = 5 mice in (O) and (P); *n* = 551 total neurons in six mice in (Q) and (R); *n* = 54 head grooming-activated cells in (T) and 42 sedated partner-activated cells in (U); *n* = 362 total neurons in five mice in (W); *n* = 32 familiar sedated partner-activated cells in (X) and 65 novel awake animal-activated cells in (Y). For (G) to (I); (M) to (O); and (T), (U), (X), and (Y); two-sided paired *t* test was performed. \*\*\*\**P* < 0.0001, \*\**P* < 0.01, \**P* < 0.05.

in the MeA have been shown to regulate several types of social behavior toward awake animals, including aggression, parenting, and allogrooming behaviors (7, 19, 20, 25), we determined whether these neurons are active during the behavior toward unresponsive mice by recording Ca<sup>2+</sup> dynamics in these neurons using fiber photometry (Fig. 5, A and B). We found that Vgat<sup>+</sup> neurons in the MeA showed an elevated Ca<sup>2+</sup> signal during head grooming behavior (Fig. 5, C to E). By contrast, these neurons did not show increased activity during self-grooming behavior (Fig. 5, F to H).

To further determine whether these neurons are required for naturally occurring head grooming behavior toward unresponsive mice, we performed optogenetic inhibition of these neurons using stGtACR2 (26) (Fig. 5, I to K). Photoinhibition in stGtACR2 animals during head grooming toward unresponsive partners led to a reduction in the duration of this behavior in an acute, time-locked manner compared with sham or fluorescent protein controls (Fig. 5, L to N). This suggests that Vgat<sup>+</sup> neurons in the MeA are required for naturally occurring head grooming behavior toward unresponsive mice. Moreover, we found that photoinhibition did not alter social investigation behavior (fig. S7, A to C), suggesting that its effect on head grooming was unlikely to result from non-specific disruption of motor movements or a decrease in general social interest.

To further test whether activation of MeA neurons is sufficient to induce head grooming behavior toward sedated animals, we optogenetically activated a subpopulation of MeA Vgat<sup>+</sup> neurons that also express the neuropeptide gene *Tac1*, which have been shown to primarily promote allogrooming toward stressed partners (7). We found that activation of these neurons increased head grooming behavior toward sedated animals in a time-

locked manner (Fig. 5, O to S). By contrast, social investigation toward sedated animals was not increased (fig. S7D). Together, our loss- and gain-of-function experiments support the notion that MeA Vgat neurons play a direct, physiological role in promoting head grooming toward sedated conspecifics.

#### Differential behavioral and neural responses toward unresponsive versus stressed social partners

Our previous research demonstrated that mice display allogrooming behavior toward awake partner animals that are stressed (7). To determine whether the behavioral responses toward unresponsive animals that we observed here simply resemble behavioral responses toward stressed animals, we performed a detailed comparison of the helpers' behaviors toward a stressed versus sedated animal (Fig. 6A). We found that whereas helper mice showed allogrooming toward both body and head areas of awake, stressed partners, most grooming behavior targeted body areas (mainly dorsal flank and neck) as opposed to head areas (Fig. 6, B to H). By contrast, helper mice exhibited substantially more time in head-directed allogrooming and less in body-directed allogrooming toward sedated conspecifics (Fig. 6, I to M). This suggests that mice were not simply treating unresponsive animals as stressed animals and that allogrooming toward unresponsive versus stressed animals represents separate behavioral responses to different states of others.

These differences in behavioral responses raise the possibility that the unresponsive and stress states of conspecifics are differentially represented in the brain. Given that MeA neural activity encodes both the unresponsive and stress states of others, we compared the neural representations of these two states in the MeA (Fig. 7A). Although there was a substantial

overlap between neurons activated by sedated or stressed conspecifics, we identified a subset of neurons that exhibited significant activation during only one type of behavior but not both (Fig. 7, B to F). Moreover, episodes of investigation toward stressed versus sedated conspecifics could be decoded by using population activity with high accuracy (Fig. 7G). These results suggest that the unresponsive and stress states of others are differentially represented in MeA neural activity. This distinction may contribute to the differential behavioral responses toward conspecifics in these two different states. Furthermore, we compared the neural representations of head grooming toward sedated animals and body grooming toward stressed animals. We found that the majority (64.6%) of cells activated during head grooming toward sedated animals were not activated during body grooming toward stressed animals and that the majority (55.6%) of cells activated during body grooming toward stressed animals were not activated during head grooming toward sedated animals (Fig. 7, H to K). Additionally, these two behaviors could be reliably distinguished using population activity in the MeA (fig. S6K). Our findings suggest that interactions with sedated versus stressed animals represent distinct social contexts and behaviors, which are differentially encoded by MeA neural activity.

#### Discussion

Humans often attend to unconscious individuals to provide care and safety. Behavioral responses toward unconscious conspecifics have also been documented in other mammalian species and may, in some cases, represent a form of attentive behavior (2–6). Yet, the characteristics and effects of this type of behavior have not been examined in experimental models under well-controlled conditions. Here, we

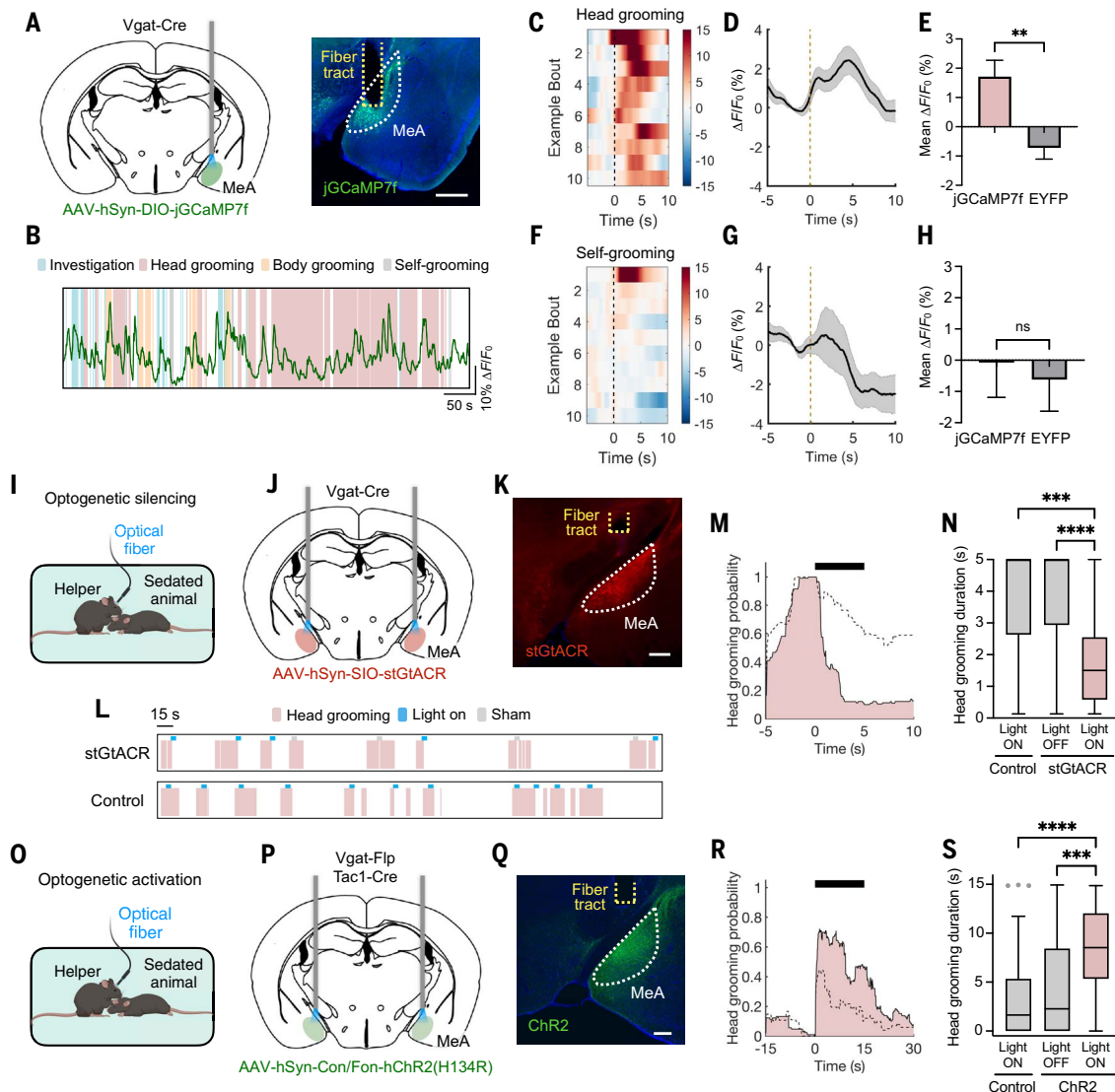


**Fig. 5. MeA GABAergic neurons control head grooming behavior toward unresponsive conspecifics.** (A) (Left) Schematic of viral injection and fiber implantation strategy for fiber photometry recording in MeA  $Vgat^+$  neurons. (Right) Example image showing viral expression in the MeA and fiber implantation site. Scale bar, 500  $\mu\text{m}$ . (B) Example raster plot of various types of behaviors displayed by helper animals overlaid with calcium fluorescence signal in MeA  $Vgat^+$  neurons. (C to H) Heatmaps showing  $\text{Ca}^{2+}$  signal changes during example bouts [(C) and (F)], average  $\text{Ca}^{2+}$  signal changes (mean  $\pm$  SEM) across all behavior bouts [(D) and (G)], and quantification of  $\text{Ca}^{2+}$  signal changes across behavior bouts (mean  $\pm$  SEM) in GCaMP and enhanced yellow fluorescent protein (EYFP) animals [(E) and (H)] during head grooming [(C) to (E)] and self-grooming [(F) to (H)] behaviors. (I) Schematic of optogenetic inhibition during interactions with sedated animals. (J) Schematic of viral injection and fiber implantation strategy for stGtACR2 inhibition of MeA  $Vgat^+$  neurons. (K) Example image showing viral expression in the MeA and fiber implantation site. Scale bar, 250  $\mu\text{m}$ . (L) Example raster plots showing head grooming toward sedated partners during real photoinhibition and sham inhibition (no laser delivery) in stGtACR2-expressing animals and during light delivery in mCherry-expressing controls. (M) Solid curve: percentage of trials showing head grooming at different time points with respect to light delivery onset (time 0) in stGtACR2 animals. Dashed curve: data from sham inhibitions (no laser delivery) in stGtACR2 animals. (N) The duration of head grooming toward sedated partners during real photoinhibition (light on) and sham inhibition (light off) in stGtACR2 animals and during light delivery in mCherry-expressing controls.

(O) Schematic of optogenetic activation during interactions with sedated animals. (P) Schematic of viral injection and fiber implantation strategy for Chr2 activation of MeA  $Vgat^+$ / $Tac1^+$  neurons. (Q) Example image showing viral expression in the MeA and fiber implantation site. Scale bar, 250  $\mu\text{m}$ . (R) Solid curve: percentage of trials showing head grooming at different time points with respect to light delivery onset (time 0) in Chr2-expressing animals. Dashed curve: data from sham stimulations in Chr2 animals. Because stimulations were delivered when the subject animals were close to sedated partners, the increased probability of head grooming at stimulation onset in the sham control group reflects baseline, naturally occurring head grooming in this behavioral context. (S) The duration of head grooming toward sedated partners during real stimulation and sham stimulation in Chr2 animals and during light delivery in EYFP-expressing controls.  $n = 56$  head grooming bouts from four GCaMP mice and 41 head grooming bouts from four EYFP (control) mice in (D) and (E);  $n = 16$  self-grooming bouts from four GCaMP mice and 29 self-grooming bouts from four EYFP (control) mice in (G) and (H);  $n = 54$  light-on trials and 41 light-off trials from six stGtACR2 mice and 96 light-on trials from eight control mice in (N);  $n = 53$  light-on trials and 44 light-off trials from five Chr2 mice and 48 light-on trials from three control mice in (S). For (E) and (H), two-sided Wilcoxon rank-sum test; for (N) and (S), Kruskal-Wallis test with post hoc Dunn's multiple comparisons test. To account for the fact that multiple trials were collected from individual animals, we also performed statistical tests using linear mixed-effects models and reached similar conclusions (see table S1). \*\*\*\* $P < 0.0001$ , \*\*\* $P < 0.001$ , \*\* $P < 0.01$ .

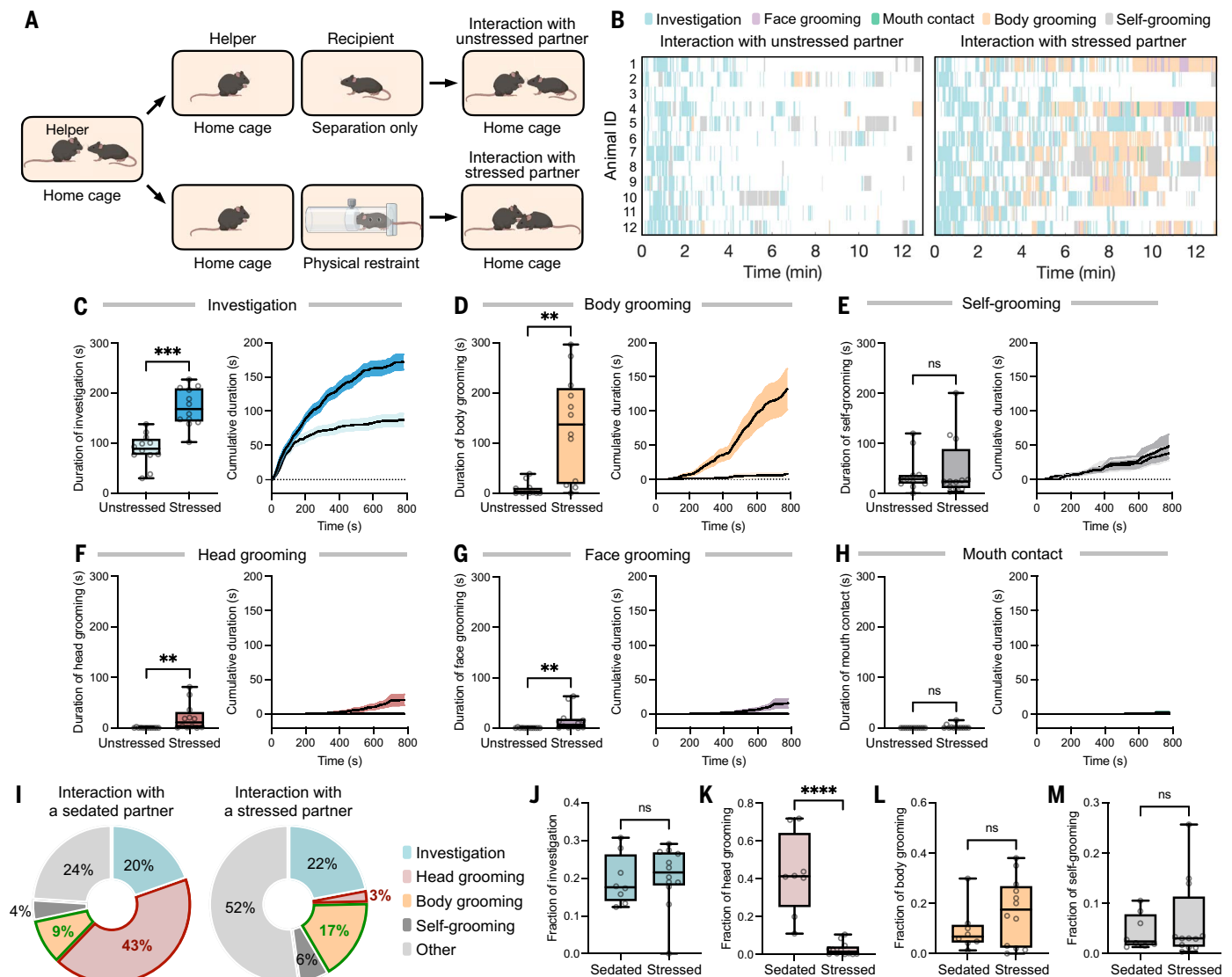


**Fig. 6. Differential behavioral and neural responses toward sedated versus stressed partners.** (A) Schematic of the behavioral paradigm for assessing social interaction with stressed partners. (B) Raster plots showing social investigation, head grooming, body grooming, and self-grooming behaviors exhibited by helper animals during interaction with unstressed or stressed partners. Each numbered row represents an individual animal. (C to H) The total durations and time courses of cumulative duration (mean  $\pm$  SEM) of various behaviors displayed by helper animals during interactions with unstressed or

stressed partners. (I) Pie charts showing the percentage of time that helper animals engaged in various types of behaviors during interactions with stressed or sedated partners. (J to M) Comparison of the percentage of time that helper animals engaged in various behaviors during interactions with stressed versus sedated partners.  $n = 12$  mice in (C) to (H);  $n = 8$  sedated mice and 12 stressed mice in (J) to (M). For (C) to (H), two-sided Wilcoxon signed-rank test; for (J) to (M), two-sided Wilcoxon rank-sum test. \*\*\*\* $P < 0.0001$ , \*\*\* $P < 0.001$ , \*\* $P < 0.01$ ; ns, not significant.

found that mice engage in rescue-like behaviors toward unresponsive conspecifics. Specifically, they display an increased social interaction toward sedated individuals compared with naive ones and exhibit intense physical contact and grooming behavior directed at the sedated individuals' head region (including facial and mouth areas) that correlates with the extent of reduction in the responsiveness of the recipients. The display of this behavior response did not appear to require visual cues, suggesting that other sensory modalities, such as somatosensory or olfactory cues, may be

involved in the detection of others' unresponsive states. The exact identity of these cues is yet to be uncovered. An interesting question is how mice distinguish between a sedated state and other normal states of immobility, such as sleep. It is possible that sedated animals may emit odor profiles distinct from those of sleeping animals. Additionally, although both sleeping and sedated animals exhibit immobility, sleeping animals can be readily aroused by external stimuli and quickly resume movement, whereas sedated animals cannot. This may provide additional cues that enable animals to distinguish

between these two states. A companion, independent study published in this issue (27) also reported a similar behavioral response toward the head region of unconscious (anesthetized) conspecifics in mice, suggesting that this behavior is generalized to various unresponsive states.

Although the effects of behaviors toward unresponsive conspecifics can be challenging to evaluate in the wild, in our experiments, we found that grooming directed at the head region of sedated mice is more likely to elicit motor responses (such as tail twitching) in the recipients compared with other behaviors. This aligns

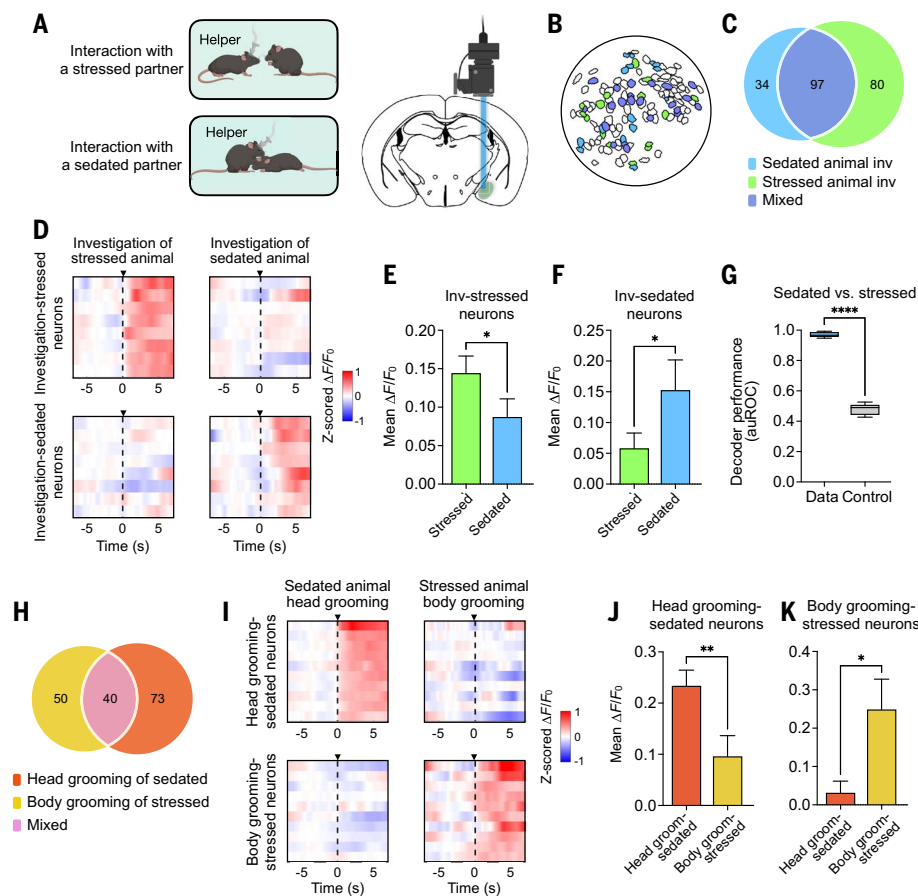


**Fig. 7. MeA encoding of interactions with sedated versus stressed partners.** (A) Schematic of the behavioral paradigm for microendoscopic imaging during interactions with stressed or sedated conspecifics. (B) Example field of view showing the spatial distribution of cells activated by stressed partners, sedated partners, or both. (C) Venn diagram showing the overlap and difference between neurons activated during social investigation toward either stressed or sedated partners. (D) Heatmaps showing average responses of example cells activated selectively during the investigation of either stressed (“Investigation-stressed neurons”) or sedated (“Investigation-sedated neurons”) partners (but not both) aligned to the onset of investigation (time 0) toward the partners. (E and F) Average activity changes (mean  $\pm$  SEM) of cells significantly activated by either stressed (E) or sedated (F) partners (but not both) during investigation toward each type of partner. (G) Performance of SVM decoders in classifying investigation events toward stressed versus sedated partners. (H) Venn diagram showing the overlap and difference between neurons activated during either head grooming toward sedated partners or body grooming toward stressed partners. (I) Heatmaps showing average responses of example cells activated selectively during either head grooming toward sedated partners or body grooming toward stressed partners (but not both) aligned to the onset (time 0) of each type of behavior. (J and K) Average activity changes (mean  $\pm$  SEM) of cells selectively activated during either head grooming toward sedated partners (J) or body grooming toward stressed partners (K) for each type of behavior. Time 0 represents the onset of behavior events.  $n = 463$  total neurons in five mice in (C);  $n = 80$  cells in (E) and 34 cells in (F);  $n = 5$  mice in (G);  $n = 408$  total neurons in four mice in (H);  $n = 73$  cells in (J) and 50 cells in (K). For (E) to (G), and (J) and (K), two-sided paired  $t$  test.

with findings from the parallel study (27) showing that the facial and mouth areas exhibit higher sensory sensitivity to mechanical stimuli. Sedated animals may also display other subtle head or body movements when receiving head grooming. It is possible that the increased motor responses of the sedated animals may provide cues that preferentially direct grooming behavior toward the face and mouth areas of the sedated animals; this remains to

be determined in future research. Notably, we found that head grooming appeared to expedite animals’ recovery from a sedated state. Thus, helper animals may exhibit intense physical contact primarily toward the head region because it is more likely to trigger motor responses and facilitate recovery. This behavior could help reduce risks to unresponsive individuals, potentially enhancing their chance of survival. Such advantages may con-

tribute to the development of this behavior through evolution.

To start to explore the neural mechanisms underlying behavioral responses toward unresponsive conspecifics, we uncovered an essential role of the MeA in regulating this process. MeA neural activity encodes the awake versus sedated state of others, and MeA GABAergic neurons bidirectionally regulate head grooming toward sedated partners. Additionally, head grooming and body grooming toward sedated animals are associated with distinguishable neural responses in the MeA. Whether these behaviors are mediated by neuronal subpopulations with distinct molecular features or connectivity awaits future investigation.

Although helper mice respond with allogrooming behavior to both conspecifics in a sedated state and awake conspecifics in a general state of stress, these responses can be separated: Allogrooming and physical contact toward unresponsive individuals was primarily focused on the head region, whereas allogrooming directed at stressed individuals was mainly targeted at other body parts. This finding suggests that mice can distinguish between these two different adverse states of others and adapt their behavior accordingly. Indeed, these two states elicit differential single-neuron and population responses in the MeA. Additionally, although both head grooming and body grooming behaviors involve the MeA, these two behaviors can be differentiated by neural activities in the MeA at both single-cell and population levels. These findings suggest that the MeA may be part of the neural circuitry mediating the differentiation between these states and the corresponding behavioral responses. Moreover, the behavioral response toward sedated conspecifics also differs from that toward conspecifics in pain, which involves allolicking behavior directed at the injury site (8, 28). Another brain area, the anterior cingulate cortex, was found to encode others’ pain state and regulate allolicking behavior in response to this state. How these distinct responses to various negative states of other individuals involve different sensory pathways and engage different neural circuits remains an interesting question for future research.

In summary, we developed an experimental model that revealed distinctive behaviors directed toward unresponsive conspecifics in mice and identified the first brain node critical for this phenomenon. These findings expand our understanding of animals’ ability to detect and behaviorally react to different adverse conditions of others and open up new avenues for investigating the neural basis of such capacities.

## Materials and methods

### Animals

Wild-type animals used in experiments were male and female C57BL/6J mice purchased at

8 to 10 weeks old from Jackson Laboratories (strain #: 000664). The Cre driver line *Vgat-ires-cre* was first purchased from Jackson Laboratories (strain #: 028862) and crossed to *C57BL/6J* to generate *Vgat<sup>Cre/+</sup>* animals. Animals were housed in a 12-hours light/dark cycle (21:00 to 9:00 light) at a temperature of 21° to 23°C with 30 to 70% humidity, with food and water *ad libitum*. Behavior experiments were performed during the dark cycle of the animals in a dark room illuminated by infrared or red light unless indicated otherwise. All experimental procedures were carried out in compliance with the NIH Guide for Care and Use of Laboratory Animals and approved by the UCLA Institutional Animal Care and Use Committee.

### Stereotaxic surgeries

10-to-12-week-old animals were anesthetized with isoflurane and mounted on a stereotaxic device (Kopf instruments). Injections were carried out using a pulled, fine glass capillary (WPI). For optogenetic inhibition experiments in the MeA, 400 nl AAV1-hSyn1-SIO-stGtACR2-FusionRed (or AAV2-EF1 $\alpha$ -DIO-mCherry as the control) was injected bilaterally in the MeA (AP: -1.65 mm, ML: +2.20 mm, DV: -5.30 mm from Bregma) of *Vgat<sup>Cre/+</sup>* mice. Ferrule fiber-optic cannulas (200- $\mu$ m core diameter, 0.37 numerical aperture; Inper) were implanted 0.50 mm above the virus injection sites. For optogenetic activation experiments in the MeA, 300 nl AAV5-hSyn-Con/Fon-nChr2(H134R)-eYFP (or AAV5-hSyn-Con/Fon-eYFP as the control) was injected bilaterally in the MeA (AP: -1.65 mm, ML: +2.20 mm, DV: -5.30 mm from Bregma) of *Vgat<sup>Fbp/+</sup>;Tac1<sup>Cre/+</sup>* mice. Ferrule fiber-optic cannulas (200- $\mu$ m core diameter, 0.37 numerical aperture; Inper) were implanted 0.45 mm above the virus injection sites. For fiber photometry experiments, 400 nl AAV1-Syn-FLEX-jGCaMP7f (or AAV2-EF1 $\alpha$ -DIO-EYFP as the control) was injected in the MeA (AP: -1.65 mm, ML: +2.20 mm, DV: -5.30 mm from Bregma) of *Vgat<sup>Cre/+</sup>* mice. Ferrule fiber-optic cannulas (200- $\mu$ m core diameter, 0.50 numerical aperture; Inper) were implanted 0.20 mm above the virus injection sites. For microendoscopic calcium imaging experiments, 400 nl AAV1-syn-jGCaMP7f-WPRE was injected in the MeA (AP: -1.65 mm, ML: +2.20 mm, DV: -5.30 mm from Bregma) of *C57BL/6J* mice. A gradient refractive index (GRIN) lens (0.6 mm; Inscopix) was implanted 0.20 mm above the virus injection site. The GRIN lens was protected with a silicon adhesive (Kwik-cast, WPI) after implantation. A baseplate was fixed above the GRIN lens 2 to 3 weeks after the surgery. AAV1-hSyn1-SIO-stGtACR2-FusionRed (Catalog # 105677-AAV1), AAV1-Syn-jGCaMP7f (Catalog # 104488-AAV1), AAV1-Syn-FLEX-jGCaMP7f (Catalog # 104492-AAV1) and AAV2-EF1 $\alpha$ -DIO-EYFP (catalog # 27056) were purchased from

Addgene. AAV5-hSyn-Con/Fon-nChr2(H134R)-eYFP, AAV5-hSyn-Con/Fon-eYFP, and AAV2-EF1 $\alpha$ -DIO-mCherry were purchased from the University of North Carolina vector core.

### Behavior assays

#### Social interaction with sedated conspecifics

The concept of sedation encompasses a continuum of responsiveness levels, ranging from minimal sedation equivalent to anxiolysis to the deepest level that is equivalent to general anesthesia (14). The extent of loss of responsiveness in sedated animals depends on the degree of sedation. In our study, animals in deep sedation exhibited minimal responsiveness, remaining mostly immobile and displaying only subtle movements (such as tail twitching) in response to external stimuli. Animals in light sedation (such as those given a lower dose of the sedative or partially recovered from sedation) exhibited more motor movements (such as small head or body movements) in response to external stimuli.

Pairs of animals (male-male, female-female, or male-female pairs) were habituated to handling procedures for at least 3 days prior to the behavioral test. One animal was assigned as the “helper” and the other one as the “partner” or “recipient.” For the interaction with an awake partner, the partner was removed from the home cage and placed in a separate cage for 15 min. For the interaction with a sedated partner, the partner was intraperitoneally injected with dexmedetomidine (0.3 mg/kg body weight; Sigma-Aldrich SML0956), and placed in a separate cage for 15 min to allow it to transition into a deep sedation state (remaining immobile in one location in either a lying or crouching posture). The partner was then reunited with the helper in the home cage, and behavior was recorded for 20 min. The starting time point for quantifying the duration of different behaviors was set as immediately after the introduction of the awake or sedated partner. The interaction with an awake partner was assessed 24 hours before the interaction with a sedated partner within the same pairs of animals.

To compare helpers’ behaviors toward sedated partners under the light versus dark condition (fig. S5, B to F), we performed the behavior assay as described above under either white-light illumination or infrared light illumination. The two sets of experiments were performed 24 hours apart on the same pairs of animals, with the order of the light and dark conditions counterbalanced across animals.

To examine the helper’s behaviors as the partner transitions from an awake to an unresponsive state (Fig. 2, A to G), the partner was intraperitoneally injected with dexmedetomidine (0.3 mg/kg body weight) and returned to the home cage to reunite with the helper immediately after injection. The behav-

ior was recorded for 20 min. The onset of the unresponsive state is defined as when the partner ceased locomotion and remained immobile in one location, adopting either a lying or crouching posture. In Fig. 2, B to D, the data were smoothed using a 20-s sliding window.

To examine helpers’ behaviors toward partners in light versus deep sedation (Fig. 2, H to N), the partner was intraperitoneally injected with dexmedetomidine at either 0.3 mg/kg body weight for deep sedation or 0.03 mg/kg body weight for light sedation, and placed in a separate cage for 15 min. The partner was then returned to the home cage to reunite with the helper, and behavior was recorded for 20 min. The two sets of experiments were performed 24 hours apart on the same pairs of animals. The order of light sedation and deep sedation was counterbalanced across animals. Male mice were used for these tests.

To examine the recovery of animals from the sedated state in the absence or presence of a cage mate (Fig. 3, G and H), the animal was intraperitoneally injected with dexmedetomidine (0.3 mg/kg body weight), and then placed in a new cage either in the absence (“alone”) or presence (“with helper”) of a helper. During deep sedation, the animals remained largely immobile, staying in one location in either a lying or crouching posture. As they gradually transitioned to wakefulness, they began to return to a standing position, displayed minor movements while staying in one location, and eventually initiated continuous exploratory movements, moving away from their initial spot. Although the transition from sedation to wakefulness is a naturally gradual process, in Fig. 3H we quantified the time it took for the animals to resume continuous movement away from their initial spot for the first time as a measure of recovery speed. The latency is calculated as the time between the intraperitoneal injection and the first continuous exploratory movement. We quantified the duration of head grooming behavior displayed by the helper animals toward the partners during the 5 min before and following recovery (fig. S5A). Male mice were used for these tests.

#### Three-chamber preference tests

Three-chamber preference tests were performed in a three-chamber apparatus consisting of two side chambers (25 cm by 25 cm) and a center chamber (12.5 cm by 25 cm). A wire cup was placed in each of the side chambers. The animal was allowed to explore the three chambers freely for 20 min, with a same-sex sedated animal under one wire cup and a same-sex awake animal under the other (Fig. 2, O and P), or with a same-sex sedated animal under one wire cup and a toy animal under the other (Fig. 2, Q and R). The chambers were assigned in a counterbalanced manner across all helper animals. The SLEAP software (<https://sleap.ai/>)

was used for behavior tracking. In one set of experiments, both the sedated and awake animals were novel to the helper mice. In another set, both the sedated and awake animals were familiar to the helper mice.

To investigate whether prior interaction with a sedated animal influences the helper's preference for that sedated animal over an awake one, the helper was first allowed to freely interact with the sedated animal for 30 min and subsequently subjected to the three-chamber test with the same sedated animal after a 90-min interval. Male mice were used for these tests.

#### *Social interaction with stressed conspecifics*

Same-sex and paired-housed animals were habituated to handling procedures for at least 3 days prior to the behavioral test. One animal was randomly assigned as the "helper" and the other one as the "partner" or "recipient." For the interaction with an unstressed partner, the partner was removed from the home cage and placed in a separate cage for 30 min. For the interaction with a stressed partner, the partner was removed from the home cage, and placed in a restrainer for 30 min. The partner was then returned to the home cage to reunite with the helper, and behavior was recorded for 13 min. The interaction with an unstressed partner was assessed 24 hours before the interaction with a stressed partner within the same pairs of animals. To compare helpers' behaviors toward stressed versus unresponsive partner (Fig. 6, I to M), the behaviors during the first 13 min of the social interactions were compared. The data were collected from experiments conducted as part of our previous study (7). Male mice were used for these tests.

Behaviors were recorded by a Point Grey Camera (FLIR) with a 15-Hz or 20-Hz sampling rate. Behaviors are manually annotated frame by frame using custom-written Python software ([https://github.com/hongw-lab/Behavior\\_Annotator](https://github.com/hongw-lab/Behavior_Annotator)). Head and body grooming behaviors were defined as visible licking and/or mouth contact localized on the head (face, mouth, and ear) and body (trunk, limb, and tail) of the other mouse (Fig. 1, C and D), respectively, during which the actor mouse shows head bobbing indicative of licking motions. Social investigation was defined as moments when a helper mouse is in proximity (within half a head length) to another mouse and orients its snout toward the other mouse to sniff.

#### *Microendoscopic calcium imaging*

##### *Behavior assays*

Male helper mice were handled and habituated for at least 3 days before experiments. For imaging during interactions with naïve, sedated, and stressed animals (Figs. 4 and 7, and fig. S6), each helper animal was presented with 1 to 4 familiar, male conspecifics in either naïve,

stressed, or sedated state, with each presentation lasting ~5 to 10 min. The stressed state was induced by physically restraining the conspecifics for 30 min. For imaging during interactions with familiar and novel conspecifics (Fig. 4 and fig. S6), each helper animal was presented with novel awake animals, familiar awake animals, novel sedated animals, and familiar sedated animals in an interleaved manner, using a total of three novel and three familiar animals. Each presentation lasted ~5 to 10 min with a ~5-min interval between presentations. Calcium fluorescence videos and behavior videos were simultaneously recorded using a miniaturized microendoscope (UCLA Miniscope v4) and a video camera, respectively. The miniscope was connected to a digital acquisition device (DAQ) through a flexible, ultra-light coaxial cable. Behavior videos were annotated by a human annotator frame by frame to identify onset and offset times of behaviors exhibited by the helper animals.

##### *Extraction of calcium signals*

Calcium fluorescence videos were recorded at 15 to 30 Hz. Raw videos from each imaging session were processed using an integrated miniscope analysis package ([github.com/etterguillaume/MiniscopeAnalysis](https://github.com/etterguillaume/MiniscopeAnalysis), [github.com/hongw-lab/Ip\\_preprocessing](https://github.com/hongw-lab/Ip_preprocessing), and [github.com/hongw-lab/Cscreener](https://github.com/hongw-lab/Cscreener)). Briefly, raw videos were first processed using the NormCorr algorithm (29) for motion correction. Motion-corrected videos were then processed using Constrained Non-Negative Matrix Factorization (CNMF-E) (23) to isolate cellular signals and associated regions of interest.  $\Delta F/F$  calcium traces of individual cells were z-scored and are presented throughout in units of standard deviation (s.d.) prior to downstream analysis.

##### *Analysis of single-cell response during behavior*

An ROC (receiver operating characteristic) analysis (7, 24) was used to identify neurons that significantly respond during each type of behavior event. A binary threshold was applied to the  $\Delta F/F$  signal to classify each time point as showing or not showing a particular behavior. The true positive rate and false positive rate of behavior detection were calculated over a range of binary thresholds spanning the minimum and maximum values of the neural signal and used to construct an ROC curve that describes how well the neural signal detects behavior events at different thresholds. The area under the AUC curve (auROC) was then calculated as a metric for how strongly neural activity was modulated by each behavior. The observed auROC was compared to a null distribution generated by circularly permuting the calcium signals by a random time shift 200 times. A neuron was considered significantly responsive ( $\alpha < 0.05$ )

if its observed auROC value exceeded the 95th percentile of this null distribution (excited if auROC > 97.5th percentile or suppressed in auROC < 2.5th percentile).

##### *Analysis of population dynamics during behavior*

For binary decoding between different types of events, support vector machine (SVM) models were used to identify hyperplanes that best separate population vectors associated with different types of events. Decoder performance was computed independently for each experiment using a leave-one-out cross-validation (LOOCV) procedure. For each experiment, the mean population activity associated with an event was considered as a sample, and samples were taken for all instances of each of the two types of events. All cells were included in the analysis. We used a hold-out sample for testing in each validation fold, while the remaining samples were used for training. To equalize the representation of training samples for each group in each fold, we randomly downsampled the group with more samples. In each fold, we first performed partial-least-square (PLS) regression on the training set with behavior type as the response variable. Next, we utilized the first  $n$  PLS components in the training data that explain at least 50% of the total variance to construct an SVM model. We then computed the first  $n$  components for the held-out sample using the loadings determined from the training set and generated a prediction score for the hold-out sample based on these components. Finally, we compared all prediction scores from all validation folds with ground truth sample labels using an ROC curve, and we used the area under this curve (auROC) as the final performance metric. The number of test samples for each group was equalized by randomly downsampling the group with more samples. The LOOCV procedure was repeated 10 times to account for the randomness during the downsampling of training and test samples. The averaged auROC was then computed across the 10 rounds. We measured the chance performance for each experiment by performing the same procedure but first circularly permuting the activity trace for each neuron. This process was repeated 20 times and the averaged auROC was calculated. For the analysis of the time course of decoding performance (Fig. 4P), SVM decoders were trained and tested using population activity at different time points relative to the true behavior onset time (ranging from 10 s before to 15 s after behavior with a 1-s interval). At each time point, samples of population activity within a 1.5-s window starting from that time point were used.

##### *Optogenetics experiments*

Following stereotaxic surgeries, the viruses were allowed to incubate for 4 to 7 weeks before

behavioral testing while animals recovered in the home cage. During the test, the partner was first separated from the helper and injected with dexmedetomidine (0.3 mg/kg body weight; Sigma-Aldrich SML0956) before being reunited with the helper. For stGtACR2 inhibition experiments, blue light generated by a 473-nm laser (CNI Laser) was manually delivered continuously for 5 s at an irradiance of  $\sim 3$  to  $10 \text{ mW mm}^{-2}$  in the target region when the helper exhibited spontaneous head grooming or investigation toward the unresponsive partner. As a control, we performed sham stimulation (no light delivery) in the same animals in the same behavioral context, with real and sham stimulations manually delivered in an interleaved manner. Additionally, we delivered light in mCherry-expressing control animals under the same behavioral conditions using the same stimulation parameters. For photo-activation experiments, light was delivered in 20-ms pulses at 20 Hz for 15 s at an irradiance of  $\sim 2$  to  $3 \text{ mW mm}^{-2}$  in the target region while the animals were in the vicinity of and oriented toward unresponsive partners. We observed head grooming in 49 of 53 stimulation trials and body grooming in 8 of 53 trials. As in the photoinhibition experiments, we also performed control trials in ChR2 animals and EYFP-expressing animals. Male mice were used for these experiments. Behaviors were manually annotated frame-by-frame using custom-written Python software ([https://github.com/hongw-lab/Behavior\\_Annotator](https://github.com/hongw-lab/Behavior_Annotator)).

### Fiber photometry

Fluorescence signals were acquired using a fiber photometry system (Doric lenses) and recorded by a Micro 1401 digitizer (CED, Cambridge, UK) using the Spike2 software (v10.09a). 460- to 490-nm light was used for excitation, and 500- to 550-nm emission light was collected. The LED power was adjusted to  $\sim 3$  to  $10 \mu\text{W}$  at the tip of the optical fiber. Behaviors were recorded by a Point Grey Camera (FLIR) with a 15-Hz sampling rate. Behaviors are manually annotated frame by frame using custom-written Python software ([https://github.com/hongw-lab/Behavior\\_Annotator](https://github.com/hongw-lab/Behavior_Annotator)) and aligned to the photometry signal.

For the analysis of the fiber photometry signal, we first corrected for photobleaching in the raw fluorescence signals over long time-scales. To this end, we first smoothed the signal over the entire session using a 1000-s moving window and then normalized the smoothed signal by its maximum value, generating drift values between 0 and 1. The drift-corrected signal was then calculated as  $F_{\text{corrected}} = F / \text{normalized drift}$ . For peri-event time histograms, time 0 was defined as the onset of a behavior. The average fluorescence between 3 and 1 s prior to the behavior onset was defined as  $F_0$  and the relative fluorescence change was

calculated as  $\Delta F/F_0 = (F - F_0) / F_0$ . Female mice were used for these experiments.

### Histology

Animals were euthanized and perfused with phosphate-buffered saline (PBS) followed by 4% paraformaldehyde (PFA). The brains were dissected out, post-fixed in 4% PFA overnight, rinsed with PBS, and bathed in 20% sucrose overnight. Brains were sectioned at 60- $\mu\text{m}$  thickness with a Leica CMI950 cryostat and imaged with a Leica DM6 B microscope.

### Quantification and statistical analysis

All statistical analyses were conducted using Prism (v10, GraphPad) or MATLAB (R2019b or R2022b, MathWorks). Details about the types of statistical tests used and sample sizes are provided in figure legends and table S1. Types of statistical tests were determined based on data distribution. *P* values were corrected for multiple comparisons when necessary. Sample sizes were not predetermined using statistical methods. Our sample sizes are similar to those used in previous publications in the field (7, 12, 30), and are deemed appropriate based on the size and statistical significance of the effects and consistency across animals. Animals of appropriate genotype, sex, age, and weight were randomly assigned to experimental or control group. Test order was counter-balanced across animals whenever necessary. Experimenters were not blind to group allocation during data acquisition or analysis. All behavioral, imaging, and optogenetics experiments were replicated in multiple animals with similar results (see figure legends for exact numbers of animals and/or trials for each experiment). Example micrographs were based on at least three independent biological samples (animals) showing similar results. The center line in the boxplots indicates the median, the box limits indicate the upper and lower quartiles, and the whiskers indicate the range from the minimum to the maximum value (Figs. 1, 2, 3, and 6, and figs. S1 to S5) or data within  $1.5 \times$  interquartile range (Figs. 4, 5, and 7, and figs. S6 and S7).

### REFERENCES AND NOTES

1. T. Cooksley, S. Rose, M. Holland, A systematic approach to the unconscious patient. *Clin. Med.* **18**, 88–92 (2018). doi: [10.7861/clinmedicine.18-1-88](https://doi.org/10.7861/clinmedicine.18-1-88); pmid: 29436445
2. M. C. Caldwell, D. K. Caldwell, "Epimeletic (Care-giving) behavior in Cetacea" in *Whales, Dolphins, and Porpoises*, K. S. Norris, Ed. (Univ. of California Press, 1966), pp. 755–790.
3. G. Bearzi, M. A. L. Reggente, "Epimeletic behavior" in *Encyclopedia of Marine Mammals*, B. Würsig, J.G.M. Thewissen, K.M. Kovacs, Eds. (Academic Press, ed. 3, 2017), pp. 337–338.
4. I. Douglas-Hamilton, S. Bhalla, G. Wittemyer, F. Vollrath, Behavioural reactions of elephants towards a dying and deceased matriarch. *Appl. Anim. Behav. Sci.* **100**, 87–102 (2006). doi: [10.1016/j.applanim.2006.04.014](https://doi.org/10.1016/j.applanim.2006.04.014)
5. M. Shimada, W. Yano, Behavioral responses of wild chimpanzees toward a juvenile that suddenly lost its animacy due to a fall accident. *Sci. Rep.* **13**, 16661 (2023). doi: [10.1038/s41598-023-43229-0](https://doi.org/10.1038/s41598-023-43229-0); pmid: 37794020

6. A. De Marco, R. Cozzolino, B. Thierry, Coping with mortality: Responses of monkeys and great apes to collapsed, inanimate and dead conspecifics. *Ethol. Ecol. Evol.* **34**, 1–50 (2022). doi: [10.1080/03949370.2021.1893826](https://doi.org/10.1080/03949370.2021.1893826)
7. Y. E. Wu *et al.*, Neural control of affiliative touch in prosocial interaction. *Nature* **599**, 262–267 (2021). doi: [10.1038/s41586-021-03962-w](https://doi.org/10.1038/s41586-021-03962-w); pmid: 34646019
8. M. Zhang, Y. E. Wu, M. Jiang, W. Hong, Cortical regulation of helping behaviour towards others in pain. *Nature* **626**, 136–144 (2024). doi: [10.1038/s41586-023-06973-x](https://doi.org/10.1038/s41586-023-06973-x); pmid: 38267578
9. C. Keyser, E. Knapska, M. A. Moita, V. Gazzola, Emotional contagion and prosocial behavior in rodents. *Trends Cogn. Sci.* **26**, 688–706 (2022). doi: [10.1016/j.tics.2022.05.005](https://doi.org/10.1016/j.tics.2022.05.005); pmid: 35667978
10. I. Ben-Ami Bartal, J. Decety, P. Mason, Empathy and pro-social behavior in rats. *Science* **334**, 1427–1430 (2011). doi: [10.1126/science.1210789](https://doi.org/10.1126/science.1210789); pmid: 22158823
11. Y. E. Wu, W. Hong, Neural basis of prosocial behavior. *Trends Neurosci.* **45**, 749–762 (2022). doi: [10.1016/j.tins.2022.06.008](https://doi.org/10.1016/j.tins.2022.06.008); pmid: 35853793
12. J. P. Burkett *et al.*, Oxytocin-dependent consolation behavior in rodents. *Science* **351**, 375–378 (2016). doi: [10.1126/science.aac4785](https://doi.org/10.1126/science.aac4785); pmid: 26798013
13. F. B. M. de Waal, S. D. Preston, Mammalian empathy: Behavioural manifestations and neural basis. *Nat. Rev. Neurosci.* **18**, 498–509 (2017). doi: [10.1038/nrn.2017.72](https://doi.org/10.1038/nrn.2017.72); pmid: 28655877
14. American Society of Anesthesiologists Task Force on Sedation and Analgesia by Non-Anesthesiologists, Practice guidelines for sedation and analgesia by non-anesthesiologists. *Anesthesiology* **96**, 1004–1017 (2002). doi: [10.1097/0000542-200204000-00031](https://doi.org/10.1097/0000542-200204000-00031); pmid: 11964611
15. T.-L. Sterley, J. S. Bains, Social communication of affective states. *Curr. Opin. Neurobiol.* **68**, 44–51 (2021). doi: [10.1016/j.cob.2020.12.007](https://doi.org/10.1016/j.cob.2020.12.007); pmid: 33434768
16. P. Chen, W. Hong, Neural Circuit Mechanisms of Social Behavior. *Neuron* **98**, 16–30 (2018). doi: [10.1016/j.neuron.2018.02.026](https://doi.org/10.1016/j.neuron.2018.02.026); pmid: 29621486
17. T. Raam, W. Hong, Organization of neural circuits underlying social behavior: A consideration of the medial amygdala. *Curr. Opin. Neurobiol.* **68**, 124–136 (2021). doi: [10.1016/j.cob.2021.02.008](https://doi.org/10.1016/j.cob.2021.02.008); pmid: 33940499
18. Y. Li *et al.*, Neuronal Representation of Social Information in the Medial Amygdala of Awake Behaving Mice. *Cell* **171**, 1176–1190.e17 (2017). doi: [10.1016/j.cell.2017.10.015](https://doi.org/10.1016/j.cell.2017.10.015); pmid: 29107332
19. W. Hong, D.-W. Kim, D. J. Anderson, Antagonistic control of social versus repetitive self-grooming behaviors by separable amygdala neuronal subsets. *Cell* **158**, 1348–1361 (2014). doi: [10.1016/j.cell.2014.07.049](https://doi.org/10.1016/j.cell.2014.07.049); pmid: 25215491
20. E. K. Unger *et al.*, Medial amygdalar aromatase neurons regulate aggression in both sexes. *Cell Rep.* **10**, 453–462 (2015). doi: [10.1016/j.celrep.2014.12.040](https://doi.org/10.1016/j.celrep.2014.12.040); pmid: 25620703
21. S. Yao, J. Bergan, A. Lanjuin, C. Dulac, Oxytocin signaling in the medial amygdala is required for sex discrimination of social cues. *eLife* **6**, e31373 (2017). doi: [10.7554/eLife.31373](https://doi.org/10.7554/eLife.31373); pmid: 29231812
22. H. Dana *et al.*, High-performance calcium sensors for imaging activity in neuronal populations and microcompartments. *Nat. Methods* **16**, 649–657 (2019). doi: [10.1038/s41592-019-0435-6](https://doi.org/10.1038/s41592-019-0435-6); pmid: 31209382
23. P. Zhou *et al.*, Efficient and accurate extraction of in vivo calcium signals from microendoscopic video data. *eLife* **7**, e28728 (2018). doi: [10.7554/eLife.28728](https://doi.org/10.7554/eLife.28728); pmid: 29469809
24. L. Kingsbury, W. Hong, A Multi-Brain Framework for Social Interaction. *Trends Neurosci.* **43**, 651–666 (2020). doi: [10.1016/j.tins.2020.06.008](https://doi.org/10.1016/j.tins.2020.06.008); pmid: 32709376
25. P. B. Chen *et al.*, Sexually Dimorphic Control of Parenting Behavior by the Medial Amygdala. *Cell* **176**, 1206–1221.e18 (2019). doi: [10.1016/j.cell.2019.01.024](https://doi.org/10.1016/j.cell.2019.01.024); pmid: 30773317
26. M. Mahn *et al.*, Efficient optogenetic silencing of neurotransmitter release with a mosquito rhodopsin. *Neuron* **109**, 1621–1635.e8 (2021). doi: [10.1016/j.neuron.2021.03.013](https://doi.org/10.1016/j.neuron.2021.03.013); pmid: 33979634
27. W. Sun, G.-W. Zhang, H. W. Tao, L. I. Zhang, Reviving-like prosocial behavior in response to unconscious or dead conspecifics in rodents. *Science* **387** (2025). doi: [10.1126/science.adq2677](https://doi.org/10.1126/science.adq2677)
28. C.-L. Li *et al.*, Validating Rat Model of Empathy for Pain: Effects of Pain Expressions in Social Partners. *Front. Behav. Neurosci.* **12**, 242 (2018). doi: [10.3389/fnbeh.2018.00242](https://doi.org/10.3389/fnbeh.2018.00242); pmid: 30386220

29. E. A. Pnevmatikakis, A. Giovannucci, NoRMCorr: An online algorithm for piecewise rigid motion correction of calcium imaging data. *J. Neurosci. Methods* **291**, 83–94 (2017). doi: [10.1016/j.jneumeth.2017.07.031](https://doi.org/10.1016/j.jneumeth.2017.07.031); pmid: [28782629](https://pubmed.ncbi.nlm.nih.gov/28782629/)
30. M. L. Smith, N. Asada, R. C. Malenka, Anterior cingulate inputs to nucleus accumbens control the social transfer of pain and analgesia. *Science* **371**, 153–159 (2021). doi: [10.1126/science.abe3040](https://doi.org/10.1126/science.abe3040); pmid: [33414216](https://pubmed.ncbi.nlm.nih.gov/33414216/)

#### ACKNOWLEDGMENTS

We thank D. Fillet for technical assistance. **Funding:** This work was supported in part by NIH grants R01-NS113124, R01-MH130941,

RF1-NS132912, and R01-MH132736 (to W.H.). **Author contributions:** F.S. performed most of the experiments; Y.E.W. performed additional experiments; F.S. and Y.E.W. analyzed data; Y.E.W. performed computational data analysis; W.H., Y.E.W., and F.S. wrote the manuscript; and W.H. supervised the entire study. **Competing interests:** The authors declare that they have no competing interests. **Data and materials availability:** All data necessary to understand the conclusions of this study are available in the main text and supplemental materials. The code used for animal behavior analysis is available at [https://github.com/hongw-lab/Behavior\\_Annotator](https://github.com/hongw-lab/Behavior_Annotator). **License information:** Copyright © 2025 the authors, some rights reserved; exclusive licensee American Association for the

Advancement of Science. No claim to original US government works. <https://www.science.org/about/science-licenses-journal-article-reuse>

#### SUPPLEMENTARY MATERIALS

[science.org/doi/10.1126/science.adq2679](https://www.science.org/doi/10.1126/science.adq2679)

Figs. S1 to S7

Table S1

Movies S1 and S2

MDAR Reproducibility Checklist

Submitted 6 May 2024; accepted 11 December 2024  
[10.1126/science.adq2679](https://doi.org/10.1126/science.adq2679)